Journal of Power Sources 188 (2009) 447–452

Contents lists available at ScienceDirect

Journal of Power Sources

journal homepage: www.elsevier.com/locate/jpowsour

Degradation of cathode current-collecting materials for anode-supported flat-tube solid oxide fuel cell

Jong-Hee Kim[a,b,1], Rak-Hyun Song[a,*], Dong-You Chung[a], Sang-Hoon Hyun[b], Dong-Ryul Shin[a]

[a] Hydrogen and Fuel Cell Research Department, Korea Institute of Energy Research, 102 Gajeong-ro, Yuseong-gu, Daejon 305-343, Republic of Korea
[b] Department of Ceramic Engineering, Yonsei University, 134 Shinchon-dong Sodaemoon-Gu, Seoul 120-749, Republic of Korea

ARTICLE INFO

Article history:
Received 22 August 2008
Received in revised form 5 November 2008
Accepted 13 November 2008
Available online 24 December 2008

Keywords:
Solid oxide fuel cell
Anode-supported flat-tube
Cathode current-collecting materials
Performance degradation
Polarization resistance

ABSTRACT

Different types of cathode current-collecting material for anode-supported flat-tube solid oxide fuel cells are fabricated and their electrochemical properties are characterized. Current collection for the cathode is achieved by winding Ag wire and by painting different conductive pastes of Ag–Pd, Pt, $La_{0.6}Sr_{0.4}CoO_3$ (LSCo), and $La_{0.6}Sr_{0.4}Co_{0.2}Fe_{0.8}O_3$ (LSCF) on the wire. Cell performance at the initial operation time is in the order of Pt > LSCo > LSCF > Ag–Pd. On the other hand, the performance degradation rate is in the order of LSCo < LSCF < Pt < Ag–Pd. LSCo paste as a cathode current-collector shows the most stable long-term performance of 0.8 V, 300 mA cm^{-2} at 750 °C, even under a thermal cycle condition with heating and cooling rates of 150 °C h^{-1}. The performance degradation of the Ag–Pd and Pt pastes is caused by increased polarization resistance due to metal particle sintering. From these results, it is concluded that a cathode current-collector composed of wound silver wire with LSCo paste is useful for anode-supported flat-tube cells as it does not experience any significant degradation during a long operation time.

1. Introduction

Solid oxide fuel cells (SOFCs) are considered to be most promising energy conversion systems due to their high efficiency, fuel flexibility, low emission of pollutants, and excellent integration with simplified reformers [1–3]. The cells can be fabricated in a variety of designs, such as tubular, planar, segmented cell in-series, monolithic, and honeycomb geometry. Among the tubular versions, options, the cathode-supported tubular design of Siemens Westinghouse is the best-known and the most developed. The cells use doped $LaCrO_3$ and Ni felt as a current-collector or interconnect, which serves as a current-passage between the cells [2,4]. In a tubular SOFC, current is conducted axially along the tube. As a result, the in-plane resistance is large due to the longer current path. The advantages of tubular designs are relatively easy gas-tight sealing, high thermal cycle resistance, a rapid response to load variation, and a rapid start-up time. Moreover, anode-supported tubular SOFCs with thin electrolyte films enable operation at reduced temperatures [5–7].

Many forms of current-collectors or interconnects exist depending on the fuel cell design. In the planar design, chromia-forming ferritic alloy and Cr-base alloy have been widely used as interconnect materials at an intermediate temperature range of 650–800 °C [1,8]. In order to reduce the contact resistance between the interconnect material and the anode, a nickel mesh was added to the anode side. On the cathode side, a cathode contacting layer was applied to the interconnect to ensure electrical contact [9]. In the tubular geometry, published reports have revealed that metal wires such as pure silver [10–12], Ni80/Cr20 [10] and Nimonic 90 [10,11] wires can be used as cathode current-collectors. Additionally, Hatchwell et al. [11,13] reported that the cell performance of an electrolyte-supported cell yields favourable performance using $LaCoO_3$-coated Nimonic 90 wire and Ag-$La_{0.2}Sr_{0.2}CrO_3$-coated Ducrolloy ($Cr5Fe1Y_2O_3$). During the 1960 s, Ag was used as cathode material and as a current-collector for a SOFC system. Due to the high volatility at 1000 °C and the large thermal expansion coefficient of silver of 25.2×10^{-6} K^{-1} [13], other cathode materials were developed. The lower operation temperature of 800 °C makes silver attractive again as a good conducting material. The vapourization of silver was also investigated by Meulenberg et al. [14]. The mass loss of silver in flowing air is higher than that in an Ar + 4 vol.% H_2 + 3 vol.% H_2O atmosphere.

If silver wire is coated with paste materials that form a conductive protection layer, the wire becomes a good current-collector for the cathode side of an intermediate temperature SOFC. In a previous study by the authors [15], an anode-supported flat-tube SOFC to increase the power density and to lower the operation temperature was designed and manufactured, and Pt wire was used as a cathode current-collector. The present work reports the results of an investigation on the degradation of cathode current-collecting

* Corresponding author. Tel.: +82 42 860 3578; fax: +82 42 860 3739.
E-mail address: rhsong@kier.re.kr (R.-H. Song).
[1] Present address: STS Research Group, Technical Research Laboratories, POSCO, Pohang, 790-785, Republic of Korea.

0378-7753/$ – see front matter © 2009 Published by Elsevier B.V.
doi:10.1016/j.jpowsour.2008.11.144

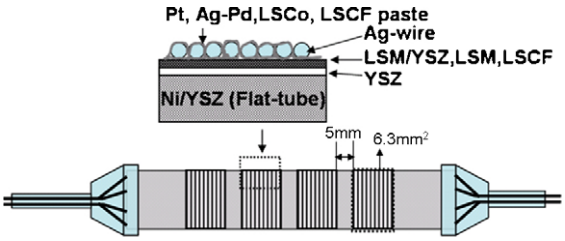

Fig. 1. Schematic of anode-supported flat-tube cells with various cathode current-collectors.

materials in an anode-supported flat-tube SOFC. For this purpose, a silver wire was wound around an anode-supported flat-tube cell as a cathode current-collector. Conductive noble-metal pastes and perovskite pastes as a current contacting layer were then painted on to the silver wire. Their electrochemical properties, long-term stability, and microstructure changes are evaluated.

2. Experimental

2.1. Preparation of anode-supported flat-tube cell

The anode-supported flat-tube was made via an extrusion process with a cermet of Ni and 8 mol% Y_2O_3-stabilized ZrO_2 (8YSZ, TZ-8Y, Tosoh co.). It was pre-sintered at 1300 °C, and an 8-YSZ electrolyte was dip-coated on the surface of the anode flat-tube and co-fired at 1400 °C [15]. The electrolyte thickness was 17 μm. A multi-layered cathode composed of a mixture of $(La_{0.85}Sr_{0.15})_{0.9}MnO_3$ (LSM) and YSZ, LSM, and $La_{0.6}Sr_{0.4}Co_{0.2}Fe_{0.8}O_3$ (LSCF) was coated on four separated cathodes of a co-sintered flat-tube, as shown in Fig. 1. The composite LSM and YSZ, LSM and LSCF layers each have a thickness of 3 μm. So, total thickness of the cathode layer is about 9 μm. The gap between the separated cathodes was 5 mm, and the cathodes were made by a slurry dip-coating process and sintered at 1200 °C. The area of each cathode was 6.3 cm^2, and this value was used to calculate the cell resistance and the power density. The prepared anode-supported flat-tube cell was joined with a ferritic stainless-steel tube (STS430, POSCO, Korea) using an induction brazing process. The latter served as a fuel gas supply [16].

Current-collection for the anode was achieved using Ni wire and felt. Current collection for the cathode was achieved by winding Ag wire with a diameter of 0.5 mm. Four different types of pastes, namely, Ag-30 wt.% Pd (Ag–Pd, Changsung Co., Korea), Pt (Tanaka Kikinzoku Kogyo K.K Co., Japan), $La_{0.6}Sr_{0.4}CoO_3$ (LSCo) and LSCF, were employed as a coating material to improve the contact between the silver wire and the cathode. The starting materials of LSCo and LSCF were synthesized by means of a solid-state reaction method and were then calcined at 1000 °C for 5 h. The powders were mixed and ground in a mortar with a binder of ethyl cellulose and an α-terpineol solvent to formulate the pastes. Finally, four different types of paste were coated with a brush on the four cathode areas wound with silver wire that were then dried in an oven at 60 °C for 3 h. A schematic diagram of the experimental set-up is shown in Fig. 1. Silver leads were attached to the four cathode sides to measure the current and the voltage.

2.2. Characterization of microstructure and electrochemical performance

The performance of the cells with four different types of cathode current-collector was measured with change in the electric load in humidified hydrogen with 3% water and air at temperatures of 750 and 800 °C. Long-term performance tests that lasted 925 h were performed at 750 °C under a constant load of 300 mA cm^{-2} or in an open-circuit state. During the long-term performance tests, a thermal cycling test was conducted twice at heating and cooling rates of 150 °C h^{-1}. The morphologies of the cathode current-collecting layer were observed using a scanning electron microscope with an energy dispersive spectroscope (SEM, JSM 6400, JEOL, Japan). Measurements of ac impedance were made with a Solartron 1260 frequency response analyzer with a Solartron 1287 electrochemical interface in the frequency range of 1×10^5 to 0.01 Hz with a 50 mV ac signal amplitude at the open-circuit state.

3. Results and discussion

3.1. Electrochemical properties of cells with different types of cathode current-collector

Fig. 2 presents the power and *I–V* performance of the anode-supported flat-tube cells with different types of cathode current-collector at operating temperatures of 750 and 800 °C after initial operation of 24 h. The cell performance depends greatly on the cathode current-collector at each operating temperature. As shown in Fig. 2(a), the cell performance is 516 mA cm^{-2} for Pt paste, 280 mA cm^{-2} for Ag–Pd paste, 419 m Acm^{-2} for LSCo paste and 330 mA cm^{-2} for LSCF paste at a cell voltage of 0.7 V. By increasing the operating temperature to 800 °C, the cell performances are increased to 380 mA cm^{-2} for Ag–Pd paste, 500 mA cm^{-2} for LSCo paste and 382 mA cm^{-2} for LSCF paste at 0.7 V. The cell with Pt paste gives the best performance of 520 mA cm^{-2} at 0.8 V, as shown in Fig. 2(b). When different types of current-collecting material are used for the cathode, the cell performance at the initial operation time is in the order of Pt > LSCo > LSCF > Ag–Pd pastes. As

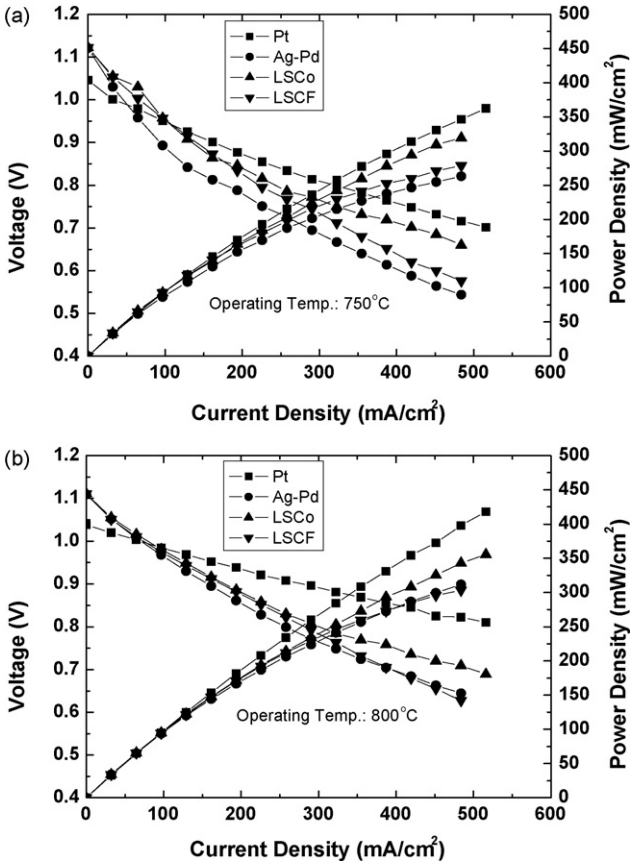

Fig. 2. Current–voltage and power densities characteristics of anode-supported flat-tube cells with various cathode current-collectors at operating temperatures of (a) 750 and (b) 800 °C.

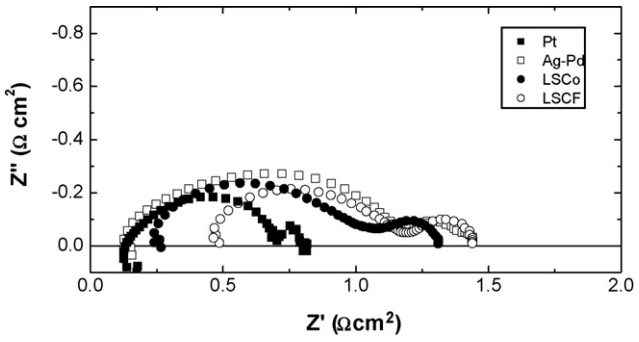

Fig. 3. Impedance spectra at open-circuit of anode-supported flat-tube cells with various cathode current-collectors at 750 °C after an initial operation of 24 h.

there are no differences in the compositions and microstructures of the electrode and electrolyte layer, the variation in performance is attributed to the cathode current-collecting layer between the wound silver wire and the surface of the cathode.

Complex impedance spectra measured at open-circuit after an initial operation of 24 h are presented in Fig. 3. The plots show two arcs; the high-frequency intercept of the arcs represents the ohmic resistance (R_o). The ohmic resistance of the cell with Pt paste is nearly identical to the resistance of the cell with Ag–Pd paste. These values are lower than those of the cell with LSCo paste or LSCF paste. The ohmic resistance contains the electrical resistances of the electrodes and electrolyte, the contact resistance between the lead wire and the electrode, and the resistance of the lead wire [10,17]. As there is no difference in the electrode structure and the electrolyte thickness, the ohmic resistance depends greatly on the contact resistance between the wound silver wire and the cathode. The polarization resistance (R_p), which were determined from impedance spectra that show two arcs, depended on the cathode current-collectors. The impedance spectra with two arcs (R_1, R_2) are interpreted as the migration and diffusion resistance (R_1) of oxygen species from the triple-phase boundary (TPB) region into the electrolyte at a high frequency, and as gaseous diffusion resistance (R_2) at a low-frequency range [18,19]. In the present work, a more precise interpretation of the dependence of the two arcs on the cathode current-collector can be made through additional experimental results; however, it is clear that these phenomena are related to the change in the cathode activity and in gas-diffusion resistance with different cathode current-collectors [20].

Table 1 lists the electrochemical properties as determined by the ac impedance and *I–V* curves at 750 °C after an initial operation of 24 h. The electrochemical performance characterized by the impedance spectra at an open-circuit state is in good agreement with the *I–V* performance characteristics at 750 °C shown in Fig. 2(a). The cell with the Pt paste shows low ohmic and polarization resistances relative to the other cells. This means that the Pt paste lowers a contact resistance between the cathode and the silver wire and increases the cathode activity. The cell with the Ag–Pd paste also demonstrates lower ohmic resistance but shows much higher polarization resistance compared with the other cells. Thus

Table 1
Electrochemical characteristics of anode-supported flat-tube cells with different types of cathode current-collectors at 750 °C after an initial operation of 24 h.

	Current density at 0.7 V (mA cm^{-2})	[a] R_{ohmic} (Ω cm^2)	[a] R_p (Ω cm^2)
Pt paste	516	0.13	0.68
Ag–Pd paste	280	0.12	1.32
LSCo paste	419	0.24	1.06
LSCF paste	330	0.46	0.98

[a] Value determined from ac impedance spectra at open-circuit.

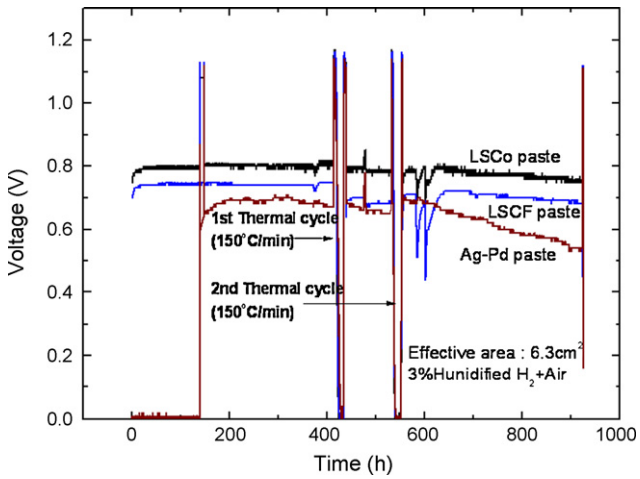

Fig. 4. Long-term performance of anode-supported flat-tube cells with various cathode current-collectors at a constant current of 300 mA cm^{-2} at 750 °C.

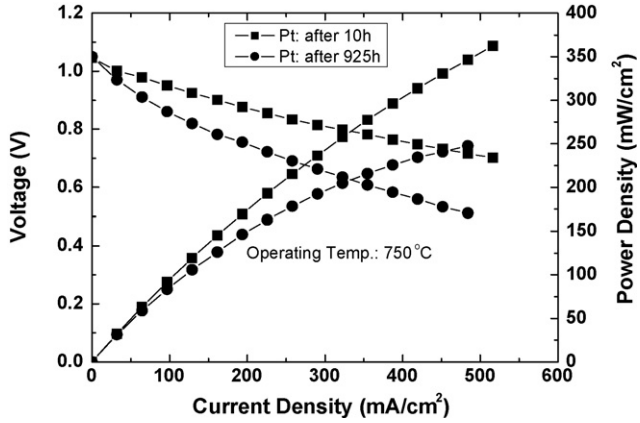

Fig. 5. Performance characteristics of anode-supported flat-tube cell with Pt paste after initial operation for 24 h and after operation for 925 h.

the performance of this cell is much lower than that of cells with either Pt or LSCo pastes. The ohmic resistance of the cell with the LSCo paste is lower than that of the cell with the LSCF paste because the electrical conductivity of the LSCo layer is higher than that of LSCF. This is consistent with the fact that the electrical conductivity, of LSCo [21], viz., 1100 S cm^{-1} is higher than that of LSCF, 350 S cm^{-1}

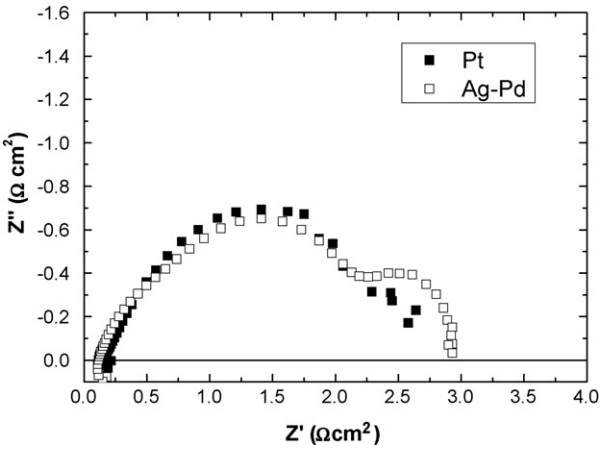

Fig. 6. ac impedance spectra for anode-supported flat-tube cells with Pt paste and with Ag–Pd paste after operation for 925 h at 750 °C.

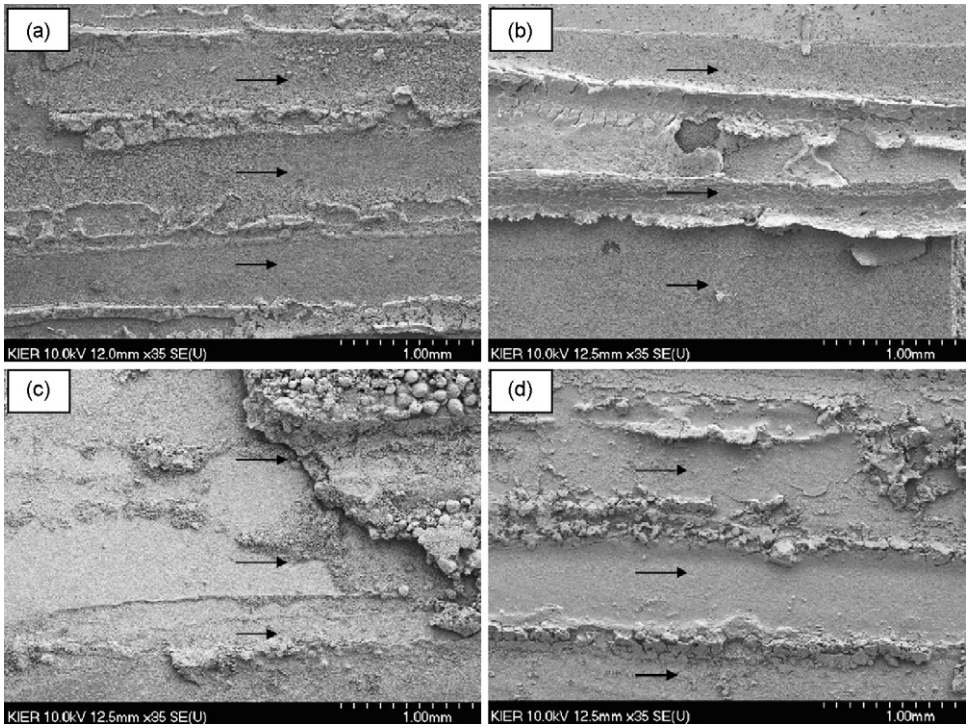

Fig. 7. SEM micrographs of cells with (a) Pt paste, (b) Ag–Pd paste, (c) LSCo paste and (d) LSCF paste after operation for 925 h (→ indicates contact surface of wound silver wire).

[22] when measured at 800 °C. On the other hand, the difference in the polarization resistance of the cell with LSCo paste and that with LSCF paste is very small. Consequently, the initial performance of the cells with LSCo and LSCF pastes is considered to depend on their conductivities.

The long-term performance of cell with Pt, Ag–Pd, LSCo, or LSCF pastes were evaluated at 750 °C under a constant current of 300 mA cm^{-2} using air as an oxidant and humidified hydrogen (3% H_2O) as a fuel. The results are shown in Figs. 4 and 5. The rate of performance degradation during a long period of operation of 925 h is in the order: LSCo < LSCF < Pt < Ag–Pd. The performance of the cell with LSCo paste increases during the initial operation time, but then remains nearly constant. With LSCo paste, significant performance degradation is not observed, even during a thermal cycling test with

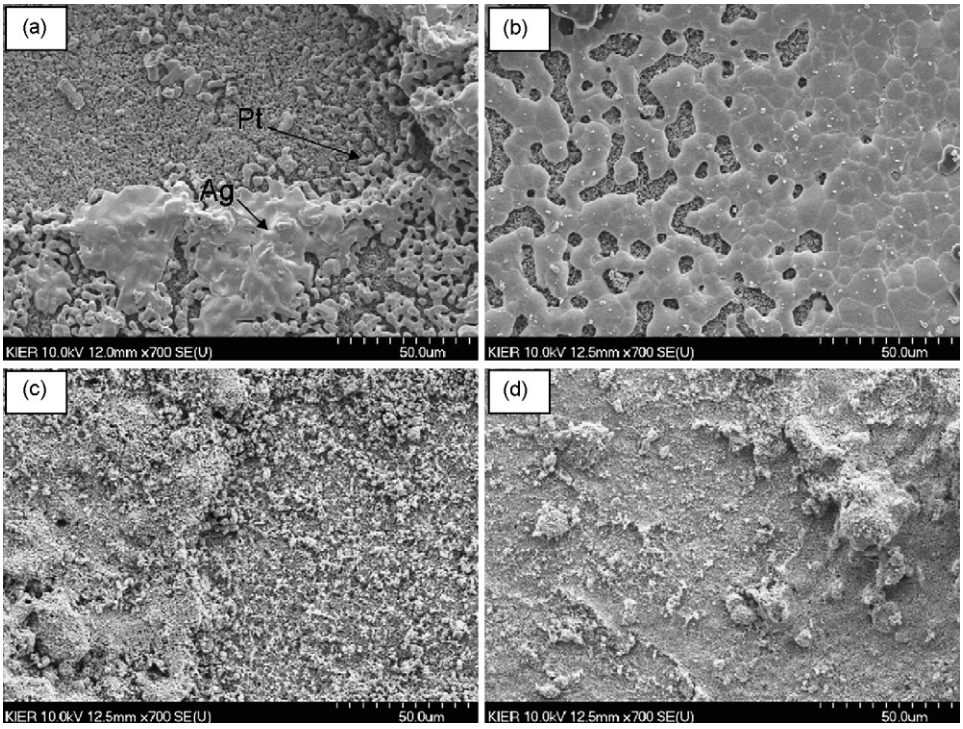

Fig. 8. Enlarged SEM micrographs of cells with (a) Pt paste, (b) Ag–Pd paste, (c) LSCo paste, and (d) LSCF paste after operation for 925 h.

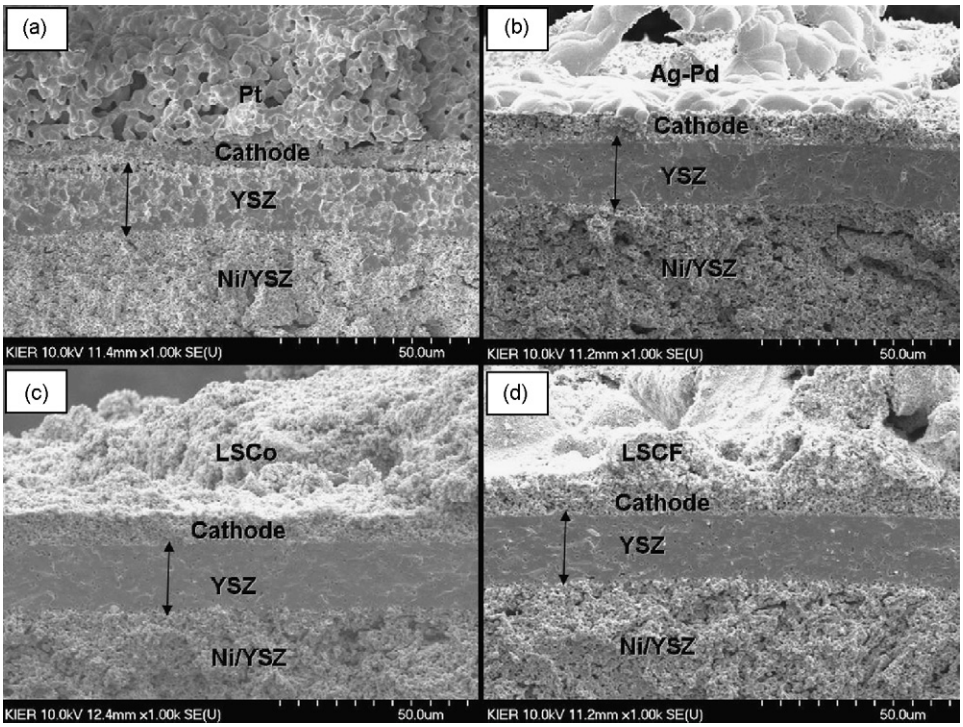

Fig. 9. Cross-section view of cells with (a) Pt paste, (b) Ag–Pd paste, (c) LSCo paste, and (d) LSCF paste.

a heating and cooling rate of 150 °C h^{-1}. With LSCF paste, slight degradation of the cell performance occurs after the first thermal cycling test, but the cell recovers after the second thermal cycling test. This is attributed to local delamination and recovery of the interface between the wound silver wire and the cathode surface during the thermal cycle.

The cell with Ag–Pd paste was held at an open-circuit state for 130 h and then subjected to a constant load of 300 mA cm^{-2} for 795 h. The long-term performance of the cell is not constant and decreases rapidly after a holding time of 600 h. The performance of the cell with Pt paste decreases from 0.82 V at an initial operation time of 24 h to 0.65 V after 925 h at 300 mA cm^{-2}, see Fig. 5. The long-term stability of this cell is not viable, which is consistent with the results reported by Yamaji et al. [19].

Fig. 6 shows the ac impedance spectra as used to analyze degradation of the performance of the cells with Pt and Ag–Pd pastes after they were operated continuously for 925 h. From a comparison of Figs. 3 and 6, the ohmic resistance (R_o) shows no change whereas the polarization resistance (R_p) increases significantly for both Pt and Ag–Pd pastes. This implies that cell degradation with Pt and Ag–Pd pastes results from an increased polarization resistance.

3.2. Microstructures of cathode current-collecting materials

Surface micrographs of each of the cathode current-collecting layers after 925 h of operation are presented in Fig. 7. The silver wires in each cell are in contact with the cathode current-collecting layers at a uniform interval, as indicated by the arrows in the Fig. 7. Enlarged micrographs of the contact surface are given in Fig. 8. Mixed phases of Ag and Pt are observed in the Pt paste, see Fig. 8(a) and the sintered particles locally cover the cathode reaction sites. The silver in the Pt-pasted current-collecting layers migrates via diffusion from the silver wire to the cathode surface during long-term operation of the cell at an operating temperature of 750 °C. The Ag–Pd pasted current-collecting layer is shown in Fig. 8(b). Sintering of the Ag–Pd particles occurs more seriously than with Pt particles. The sintered Ag–Pd current-collecting layer locally covers much of the cathode surface area, which decreases oxygen diffusion to the cathode reaction site and lowers the overall cell performance. On the other hand, the LSCo and LSCF pasted layers, as shown in Fig. 8(c) and (d), are more porous than the Pt and Ag–Pd pasted layers even after long-term operation. Additionally, silver diffusion from the silver wire into these perovskite-pasted cathode surfaces is not observed, resulting in a stable gas path and cathode reaction sites.

Fig. 9 shows cross-section images of cells with different types of cathode current-collecting layer after operation for 925 h. The microstructures are in good agreement with those of Fig. 8. The morphology of the cell with a Pt pasted current-collecting layer shows moderate porosity with a somewhat dense layer and good electrical connection. A much denser layer is formed in the Ag–Pd pasted current-collector, which limits oxygen diffusion to the cathode as shown in Fig. 9(b). From the data in Figs. 8 and 9, the increased polarization resistance of cells with Pt and Ag–Pd pastes in Figs. 3 and 6 after long operation is attributed to lack of oxygen diffusion to the cathode due to the formation of a dense layer. The LSCo and LSCF pasted current-collecting layers in Fig. 9(c) and (d) are still porous after long operation. These stable porous structures allow sufficient oxygen diffusion to the cathode reaction site, which protects against degradation of cell performance during long operation. Therefore, although current-collecting pastes increase the cell performance on initial operation, the sintering of the current-collecting materials during long operation should not be prevented to avoid degradation of the cell performance.

4. Conclusions

The effect of cathode current-collecting materials on the performance characteristics of anode-supported flat-tube cells has been investigated. The materials are prepared by coating four different types of paste on wound silver wires. The cell performance, electrochemical properties (via impedance spectroscopy) and microstructures are evaluated. The cell coated with LSCo paste

gives the highest performance and best long-term stability, even after two thermal cycling tests. The cell with LSCF paste provides relatively low performance due to its high ohmic resistance compared with the cell with LSCo paste. On the other hand, the initial performance of the cell with Pt paste is better but rapid degradation of cell performance ensued after 925 h due to an increase in polarization resistance. The cell with Ag–Pd paste displays the poorest performance and long-term stability due to the formation of a dense pasted layer at an operating temperature of 750 °C.

References

[1] N.Q. Minh, Takehiko, Science and Technology of Ceramic Fuel Cell, Elsevier Science, Amsterdam, 1995.
[2] U.S. Department of Energy, Office of Fossil Energy, National Energy Technology Laboratory, Fuel Cell Hand Book, Seventh ed., EG&G Technical Services, Inc., 2004.
[3] S.C. Singhal, K. Kendall, High Temperature Solid Oxide Fuel Cells: Fundamentals, Design and Applications, Elsevier Science, Amsterdam, 2003.
[4] W. Rauch, K.J. Lee, J. Cocharan, M. Liu, in: S.C. Singhal, M. Dokiya (Eds.), Proceedings of the 8th International Symposium on Solid Oxide Fuel Cells, 2003–07, The Electrochemical Society, Pennington, NJ, USA, 2003, pp. 1090–1100.
[5] R.H. Song, E.Y. Kim, D.R. Shin, H. Yokokawa, in: U. Stimming, S.C. Singhal, H. Tagawa (Eds.), Proceedings of the 6th International Symposium on Solid Oxide Fuel Cells, 99–19, The Electrochemical Society, Pennington, NJ, USA, 1999, pp. 845–850.
[6] R. H. Song, D. R. Shin, E. Y. Kim, H. Yokokawa, U.S. Patent 6,436,565 B1, 2002, in press.
[7] N.M. Sammes, Y. Du, R. Bove, J. Power Sources 145 (2005) 428–434.
[8] W.J. Quadakkers, T. Malkow, J. Piron-Abellan, U. Flesch, V. Shemet, L. Singheiser, in: J. McEvoy (Ed.), Proceedings of the 4th European Solid Oxide Fuel Cell Forum, European SOFC Forum, 2000, pp. 827–836.
[9] U. Flesch, R. Dahl, R. Peters, D. Stöver, in: S.C. Singhal, M. Dokiya (Eds.), Proceedings of the 6th International Symposium on Solid Oxide Fuel Cells, 99–19, The Electrochemical Society, Pennington, NJ, USA, 1999, pp. 612–620.
[10] I.P. Kilbride, J. Power Sources 61 (1996) 167–171.
[11] C.E. Hatchwell, N.M. Sammes, K. Kendall, J. Power Sources 70 (1998) 85–90.
[12] K. Kendall, M. Palin, J. Power Sources 71 (1998) 268–270.
[13] C. Hatchwell, N.M. Sammes, I.W.M. Brown, K. Kendall, J. Power Sources 77 (1999) 64–68.
[14] W.A. Meulenberg, O. Teller, U. Flesch, H.P. Buchkremer, D. Stover, J. Mater. Sci. 36 (2001) 3189–3195.
[15] J.H. Kim, R.H. Song, K.S. Song, S.H. Hyun, D.R. Shin, H. Yokokawa, J. Power Sources 122 (2003) 138–143.
[16] J. H. Kim, R. H. Song, D. R. Shin, J. Fuel Cell Sci. Technol., in press.
[17] M. Guillodo, P. Vernoux, J. Fouletier, Solid State Ionics 127 (2000) 99–107.
[18] T.L. Nguyen, T. Honda, T. Kato, Y. Iimura, K. Kato, A. Negishi, K. Nozaki, M. Shiono, A. Kobayashi, K. Hosoda, Z. Cai, M. Dokiya, J. Electrochem. Soc. 151 (2004) A1230–A1235.
[19] K. Yamaji, H. Kishimoto, Y. Xiong, T. Horita, N. Sakai, H. Yokokawa, Solid State Ionics 175 (2004) 165–169.
[20] S.P. Jiang, J.G. Love, Y. Ramprakash, J. Power Sources 110 (2003) 201–208.
[21] H.Y. Jung, W.S. Kim, S.H. Choi, H.C. Kim, J. Kim, H.W. Lee, J.H. Lee, J. Power Sources 155 (2006) 145–151.
[22] A. Mineshige, J. Izutsu, M. Nakamura, K. Nigaki, J. Abe, M. Kobune, S. Fujii, T. Yazawa, Solid State Ionics 176 (2005) 1145–1149.